Applied Magnetic Resonance (2025) 56:1489–1498
https://doi.org/10.1007/s00723-025-01814-8

Applied
Magnetic Resonance

RESEARCH

Development of Cylindrical Resonator for Millimeter-Wave Band ESR/NMR Double Magnetic Resonance

Yuya Ishikawa[1] · Kenta Ohya[1] · Kohei Hirozawa[1] · Jarno Järvinen[2] · Sergey Vasiliev[2] · Yutaka Fujii[1]

Received: 16 September 2025 / Revised: 8 October 2025 / Accepted: 9 October 2025 /
Published online: 25 October 2025

Abstract

We have developed a magnetic resonance equipment for low temperature and high magnetic fields, aiming at Dynamic Nuclear Polarization-Nuclear Magnetic Resonance (DNP-NMR) and Electron-Nuclear DOuble Resonance (ENDOR) of diluted spin system using with electron spin resonance (ESR). In this study, we developed a cylindrical resonator with a submicron-thick gold film for millimeter-wave band ESR/NMR double magnetic resonance by exploiting the frequency dependence of the skin depth. ESR measurements were performed using the fabricated resonator at approximately 130 GHz and in the temperature range of 3–70 K of BDPA diluted to 100 mM in polystyrene. ESR sensitivity was obtained from the measurements. The ^{19}F-NMR signal from the sample holder was also successfully observed.

1 Introduction

Nuclear magnetic resonance (NMR) and electron spin resonance (ESR) are widely used methods for investigating the basic magnetism of substances from a microscopic perspective. NMR measures the response of nuclear magnetic moments, which provides information on the structure of organic compounds and dynamics of surrounding electron spins [1, 2]. The ESR technique can provide information on the environment of unpaired electrons which gives g value, as well as information on electron–electron or electron–nuclear spin interactions [3–5]. ESR and NMR are generally performed independently because of the difference in the

✉ Yuya Ishikawa
ishikawa@fir.u-fukui.ac.jp

[1] Research Center for Development of Far-Infrared Region, University of Fukui, 3-9-1 Bunkyo, Fukui 910-8507, Japan

[2] Wihuri Physical Laboratory, Department of Physics and Astronomy, University of Turku, Turun Yliopisto, 20014 Turku, Finland

measurement targets. In recent years, with the progress of high-frequency light sources, the development of measurement methods that combine ESR and NMR has attracted much attention, especially in dynamic nuclear polarization (DNP)-NMR measurement methods [6–9]. It has been reported that the sensitivity of NMR measurement is improved due to the DNP effect caused by irradiation of the millimeter wave of ESR frequency on the substance with hyperfine structure which is the interaction between electron and nucleus [10–14]. This method can improve NMR sensitivity especially for systems with dilute or small magnetization of nuclear spins. However, to perform this measurement, the ESR frequency must be known in advance. Most of DNP–NMR measurement system that have been developed so far have been designed to maximize NMR sensitivity without capability of ESR measurements.

It is generally known that the NMR sensitivity largely depends on the filling factor of the sample in the oscillating magnetic field created by the RF coil. To perform highly sensitive DNP–NMR measurement, it is necessary to bring the sample as close to the coil as possible without disturbing the millimeter-wave mode for ESR. We have developed an ESR/NMR resonator in which a Helmholtz-type coil for NMR was installed in a Fabry–Pèrot-type resonator (FPR) for ESR, for planar samples [15–17]. This arrangement is useful for electron–nuclear double resonance (ENDOR) measurements because of the high sensitivity of ESR measurements. However, because the spatial arrangement of the Helmholtz type coil is limited to avoid disturbing the millimeter-wave mode in the FPR, the filling factor of the sample for NMR cannot be high. Several years ago, two examples of ESR/NMR resonators with a cylindrical shape were reported [18, 19]. In this double-magnetic-resonance resonator, a solenoid coil with a strip of conductor for NMR also serves as a cylindrical resonator for ESR at approximately 140 GHz using the TE_{011} electromagnetic wave mode. Weis et al. reported the measurement results of ^{13}C NMR signal and ^{2}H Mims-ENDOR enhanced by the DNP effect using this resonator. This resonator shape has the advantages that the filling factor of the sample in the coil for NMR can be as high as that for a normal solenoid, and that one resonator can provide multimode for ESR, while the Q value (Quality value) of the resonator for ESR is deteriorated because the millimeter wave leaks between the turns of the coil. This low Q value is acceptable for pulsed ESR/ENDOR methods, such as Mims-ENDOR. However it is disadvantageous for cw-ESR measurements and for efficient irradiation of incident microwave power for DNP. It is favorable if one can measure in cw-ESR with an ESR/NMR double resonator for precise tuning of the ESR frequency for DNP measurements. In this study, to improve the sensitivity of DNP-NMR, we developed a cylindrical resonator using a thin film made of gold (Au) that takes advantage of the different skin depths of ESR and NMR frequencies. By making an Au thin film with a thickness that reflects millimeter waves and transmits radio-frequency (RF) waves inside the resonator made of insulator resin. In other words, this means stopping the leakage of millimeter waves. This idea of utilizing gold layer to realize a resonator for ESR/NMR double magnetic resonance has already been used for a FPR [16, 17, 20]. Here, we report the development of a cylindrical type

resonator for the ESR/NMR double magnetic resonance and the results of NMR and ESR measurements.

2 Principle and Experimental

2.1 Relation Between Shape of Cylindrical Resonator and Resonance Frequency

The design of the resonator needs to fully consider the magnetic field and electric field patterns of various electromagnetic modes, that is, the H and E fields in the cavity and the current distribution I in the cavity wall. If the patterns are carefully considered, unnecessary modes can be suppressed and the desired modes can be excited. Furthermore, it is possible to effectively position the sample insertion position and appropriately set the sample insertion hole into the cavity and electromagnetic wave insertion hole (iris). The resonance condition equation for the cylindrical resonator is given by the following equation [3],

$$(Df)^2 = \left(\frac{cX_{l,m}}{\pi}\right)^2 + \left(\frac{nc}{2}\right)^2\left(\frac{D}{L}\right)^2, \tag{1}$$

where f is the resonance frequency, c is the speed of light, and D and L are the diameter and the length of the cylinder, respectively. l, m, and n are integers representing the electromagnetic wave mode TE_{lmn}, and $X_{l,m}$ is m-th root of the l-th order Bessel function J_l'. For TE_{0mn} modes of a cylindrical resonator, the quality factor Q representing the sharpness of resonance has a broad maximum as a function of D/L ratio around $D/L = 1$.

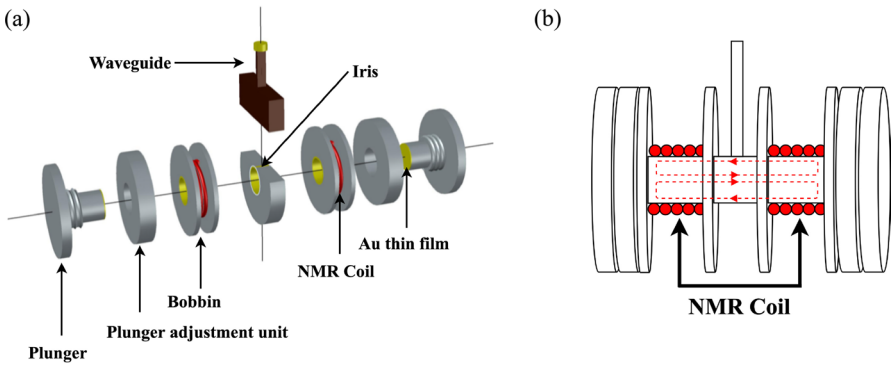

Fig. 1 **a** Schematic of a cylindrical resonator using Au thin film. **b** Cross-sectional view of the magnetic field distribution in the resonator (red dotted line, assuming TE_{011} mode magnetic field distribution)

2.2 Cylindrical ESR/NMR Dual Magnetic Resonance Resonator Using Au Thin Film

In this subsection, the resonator for double magnetic resonance developed in this research is explained (Fig. 1a). This resonator uses the TE_{015} mode and the oscillating magnetic field distribution becomes maximum at the center of the cylinder axis (Fig. 1b). Plungers at both ends of the resonator can change the length L of the cylindrical cavity, by which the resonance frequency can be adjusted accordingly. The screw pitch was 1 mm. The base material of the cylindrical resonator was polyether ether ketone (PEEK), which is a highly insulating resin material and oxygen-free copper is used for the coupling with the waveguide. The NMR coil was wound along the outside of the PEEK material. The Au thin film was sputtered onto the inner wall of the resonance part using a coater (SC-701Mk II Advance, Sanyu Electron Co., Ltd). The deposited film thickness is estimated to be 0.47 μm from the sputtering time. The thickness of this Au thin film corresponds to a skin depth range (calculated as 0.22–6.7 μm) that reflects millimeter waves for ESR (approximately 128 GHz) while transmitting radio waves for NMR (approximately 138 MHz). Consequently, the film reflects millimeter waves and transmits high-frequency waves.

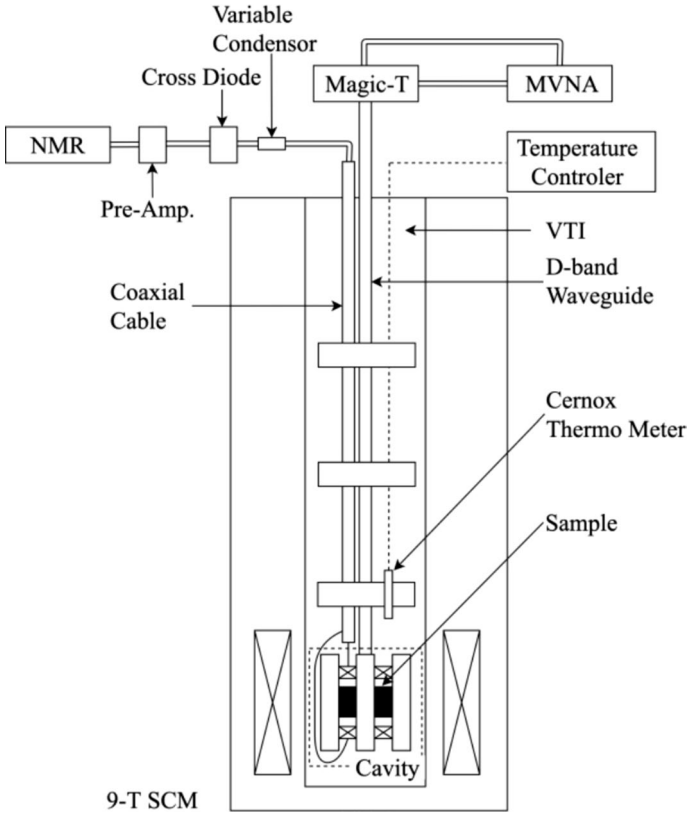

Fig. 2 Schematic diagram of a cryogenic ESR and NMR system with a cylindrical resonator

2.3 ESR/NMR System

Here, we describe the cryogenic ESR/NMR measurement system used for measurements in the following section. Figure 2 shows the ESR/NMR measurement system used in this study. A Millimeter Vector Network Analyzer (MVNA) (Model MVNA8-350–2, manufactured by ABmillimetre) was used as both the light source and detection system. The magnetic field was generated by a 9-T superconducting magnet (9-T SCM, Oxford Instruments) with the magnetic field homogeneity of 10^{-5}/10 mm DSV. The sample was cooled with a variable temperature insert (VTI, Oxford Instruments). The usable temperature range of VTI is 1.5–200 K. A Cernox resistance thermometer of CX series (Lake Shore Cryotronics, Inc.) was installed just above the resonator to measure the temperature of the sample. We performed cw-ESR by measuring the reflected power from the resonator while sweeping the magnetic field.

We used a conventional pulsed NMR measurement system that is almost identical to that described elsewhere [21] except that the resonance circuit was not be installed in the cryogenic part. Alternatively, we utilized a top-tuning system in which the capacitance of a variable capacitor and the length of coaxial cable connected to the coil on the resonator were adjusted at outside of the cryostat.

3 Results and Discussion

3.1 Manufacture and Resonance Characteristics of a Cylindrical Resonator

As shown in Eq. (1), the resonance frequency of the cylindrical resonator strongly depends on the diameter D and the length L of the cavity. Furthermore, in a high frequency range above 100 GHz, high processing accuracy is required because the wavelength becomes short. The base material of the resonator must be an insulating material. In this study, PEEK resin, which has higher strength and heat resistance than STYCAST1266, was used. The inner diameter D of the resonator was φ 6.5 mm, and the length L could be adjusted within the range of 4.4–8.9 mm. The diameter of the iris was φ1 mm. The developed cylindrical resonator uses the TE_{015} mode and is designed with a resonance frequency of 128 GHz. To prevent the mixing of unwanted resonance modes. The resonator body was sliced into a few parts and the plunger diameter was made to be φ 6.2 mm which is a little smaller than D. This increases electrical resistance between the parts and suppresses the TM mode in which current flows in the longitudinal direction of the cylinder [3]. The resonance characteristics of the cylindrical resonator was measured at room temperature using an MVNA. The measurement method was identical to that described in our previous study [16]. As shown in Fig. 3a, a resonance mode was observed at a frequency of 127.51 GHz, and the Q value of this mode was estimated to be about 6500. The waves of the background are attributed to standing waves in a waveguide used to connect between MVNA and the resonator. Moreover, it was confirmed that the resonance frequency can be adjusted by moving the plungers as shown in

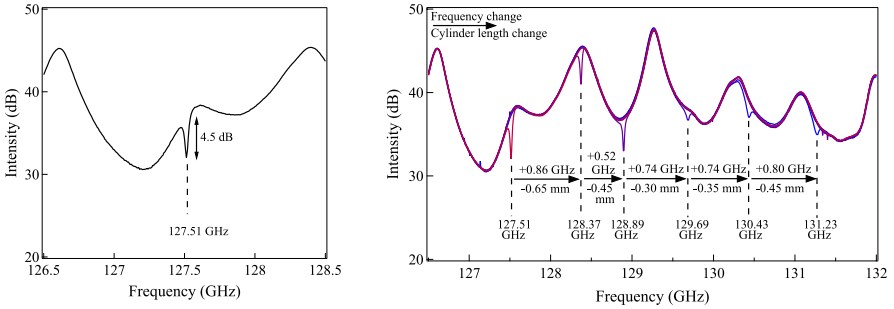

Fig. 3 **a** Observation result of resonance at frequency 127.5 GHz measured using an MVNA. **b** Frequency sweeps for several values of distance L between plungers showing resonance frequency adjusted by moving the plunger position. The amount of change in L and frequency for each step is shown. The resonance frequency increased with decreasing L

Fig. 3b. As expected, the resonance frequency increased as the distance between the plungers which equals L was decreased. The reason why the change in resonant frequency is not proportional to the change in L is probably due to the rattling of the screw that fixes the plunger. Such processing accuracy also affects Q value because the accuracy of parallelism between the plunger surfaces is important for TE_{01n} modes.

3.2 ESR Measurement

To evaluate the developed resonator, ESR measurement of BDPA radical (α,γ-bisdiphenylene-β-phenylallyl) diluted to 100 mM in polystyrene was performed. The BDPA radical is a stable organic radical molecule and its crystal is known to have a sharp ESR line [22, 23]. BDPA is also utilized as a donor electron spin for causing ESR in DNP-NMR measurement [24]. Therefore, BDPA is suitable for evaluation in this study. Since this sample has one radical per molecule and the spin number can be adjusted by the dilution concentration, it can be used for a sensitivity evaluation. Figures 4, 5 and 6 show the temperature dependences of the ESR spectrum, the integrated intensity of the ESR line, and the resonance frequency of the resonator, respectively. At each temperature, the ESR measurement frequency was adjusted to the resonant frequency of the resonator. Note that each measurement error in Figs. 5 and 6 is within the marker.

At approximately 130.85 GHz, one ESR line was observed over the entire temperature range from 5 to 70 K. The ESR spectrum at each temperature was averaged over five sweeps. For the ESR spectrum at 5 K, the half- width at half-maximum was obtained to be 2 mT (=20 G), and the signal-to-noise ratio (S/N ratio) was 6. No anomalies associated with the magnetic phase transition were observed in the temperature dependence of the integrated intensity, suggesting that it was paramagnetic in this temperature region. Regarding the temperature dependence of the resonance frequency, it was found that the resonance frequency increased as the temperature decreased. This is due to the contraction of the resonator. Next, the ESR

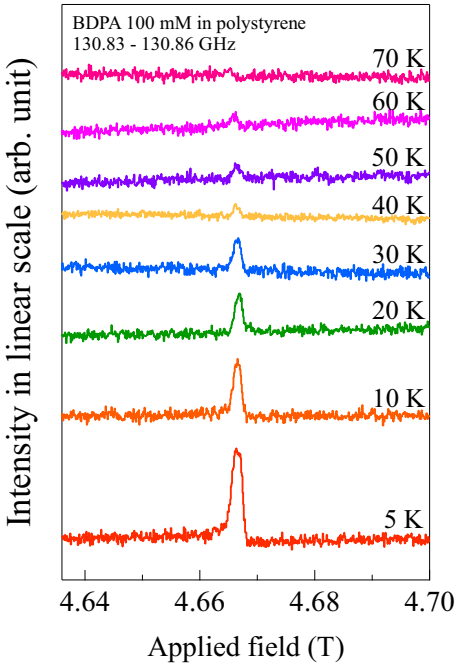

Fig. 4 Temperature dependence of ESR spectrum of BDPA 100 mM in polystyrene. The intensity is shown in a linear scale. Each spectrum is shifted vertically for clarity

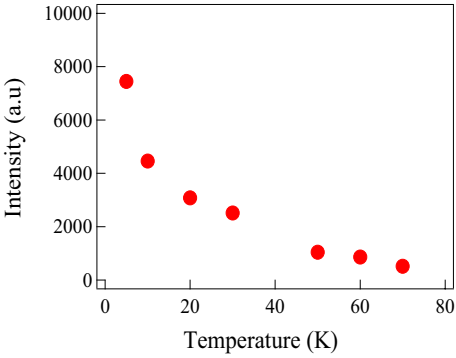

Fig. 5 Temperature dependence of integrated intensity of ESR line

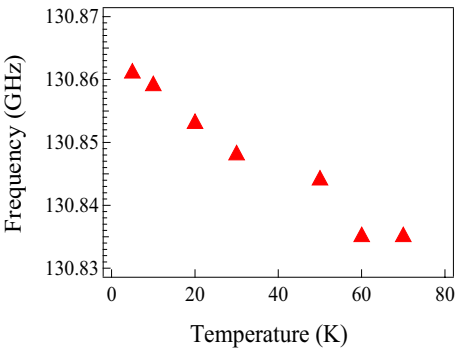

Fig. 6 Temperature dependence of resonance frequencies

measurement sensitivity of the resonator developed in this research is estimated. The measurement sensitivity of ESR can be expressed as the number of spins observable per Gauss. Considering that the sample used in this experiment was 34.66 mg and the density of the diluted polystyrene was 1.05×10^3 g/L, the number of spins contained in the sample was 2.0×10^{18} spins. The measurement sensitivity at about 5 K was calculated by (the number of spins)/((half-width)×(S/N ratio)), and was obtained to be 2×10^{16} spins/G.

3.3 $T^{19}F$-NMR Measurement

NMR measurement were performed at 7 K using the developed cylindrical resonator with the same sample as that used in the ESR measurements. The measurements were performed with 117.55 MHz under the magnetic field 2.79 T, targeting ^{19}F contained in a sample holder tube made of Teflon to prove that we can detect NMR signal of the sample inside of the resonator. The Fourier Transform (FT) spectrum of obtained ^{19}F-NMR spin-echo signal is shown in Fig. 7. Here, the pulse width was 5 μs and the signal was averaged for eight times. The practicality of the cylindrical resonator on NMR measurement in the low temperature region was confirmed. It is noteworthy that the sensitivity of NMR is possibly improved if the thickness of the Au film can be reduced without losing ESR sensitivity. The optimization of the film thickness is a future challenge.

4 Summary

In this research, we developed a cylindrical resonator for double magnetic resonance of ESR/NMR to increase the sensitivity of DNP-NMR in the high frequency and low-temperature regions. The resonator was made of PEEK with a submicron-thick gold film on the inner wall. This film thickness is such that the millimeter wave for ESR is reflected inside the resonator and the NMR RF wave generated by the coil wound outside the resonator is transmitted across the film due to the frequency dependence of the skin depth. The Q value representing the

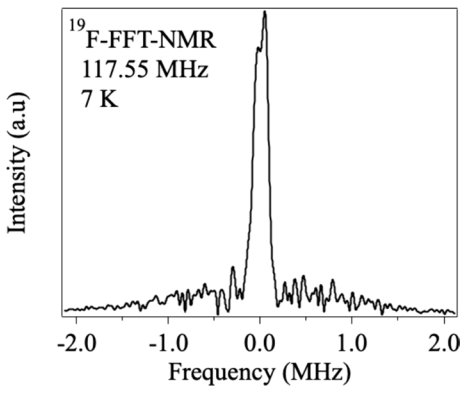

Fig. 7 ^{19}F-FT-NMR spectrum at 7 K

sharpness of resonance was estimated to be 6500 at 127.5 GHz for a designed mode TE_{015}. The frequency was variable at least in a range of 127.5–131.2 GHz at room temperature by moving the plungers at both ends of the resonator. As an evaluation in ESR, BDPA radical diluted in polystyrene at a concentration of 100 mM, was measured in the temperature range of 5–70 K and in the vicinity of 130.85 GHz. The ESR measurement sensitivity was estimated to be 1.8×10^{16} spins/G. As an evaluation in NMR, the NMR signal of ^{19}F contained in a Teflon sample holder tube put in the resonator was observed at 7 K and 117.55 MHz. These results show that both ESR and NMR signals were successfully obtained at very low temperatures using the cylindrical resonator made of submicron-thick gold film. From this result, the developed cylindrical resonator can be used for ESR/NMR dual magnetic resonance in high frequency and low temperature region with keeping acceptable sensitivities both for cw-ESR and for pulsed NMR. Better sensitivity will be possibly obtained by optimizing the thickness of the gold film and improving the processing accuracy.

Acknowledgements One of the authors (Y. I.) would like to thank to Mr. Hidetomo Yamamori and everyone at the Advanced Development Center, University of Fukui, Dr. Takashi Furuya at Research Center for Development of Far-Infrared Region, University of Fukui, and Prof. Akira Fukuda at Hyogo College of Medicine for their technical support and useful discussions in carrying out this research.

Author Contributions Yuya Ishikawa wrote the main manuscript text and prepared all of the figures and did all of these experiments. Yutaka Fujii gave us his foundation and did the experiment with Yuya Ishikawa. Kenta Ohya designed and fabricated the cavity and did the basic experiments. Kohei Hirosawa did the NMR measurements and measured resonant property. Jarno Järvinen and Sergey Vasiliev gave us the comments and support data for development of this cavity. They contributed to the succeeding the development.

Funding Open Access funding provided by University of Fukui.

Data Availability No datasets were generated or analysed during the current study.

Declarations

Conflict of interest The authors declare no competing interests.

References

1. C.P. Slichter, *Principles of Magnetic Resonance*, 3rd edn. (Springer-Verlag New York, 1990)

2. A. Abragam, *The Principles of Nuclear Magnetism* (Clarendon Press, Oxford, 1961)
3. C.P. Poole Jr., *Electron Spin Resonance*, 2nd edn. (Dover Publishing, 1997)
4. A. Abragam, B. Bleaney, *Electron Paramagnetic Resonance of Transition Ions* (Dover Publications, 1986)
5. R.S. Alger, *Electron Paramagnetic Resonance: Techniques and Applications*, 2nd edn. (John Wiley & Sons Inc., New Jersey, 1968)
6. A.W. Overhauser, Phys. Rev. **92**, 411 (1953)
7. T.R. Carver, C.P. Slichter, Phys. Rev. (1956). https://doi.org/10.1103/PhysRev.102.975
8. T. Maly et al., J. Chem. Phys. **128**, 052211 (2008)
9. Y. Matsuki et al., J. Infrared Milli Terahertz Waves. **33**, 745–755 (2012)
10. L.R. Becerra et al., Phys. Rev. Lett. (1993). https://doi.org/10.1103/PhysRevLett.71.3561
11. V. Vizthum et al., J. Magn. Reson. **205**, 177–179 (2010)
12. Y. Fujii et al., J. Phys. Conf. Ser. **568**, 042005 (2014)
13. J. Järvinen et al., Phys. Rev. B **90**, 214401 (2014)
14. J. Järvinen et al., Phys. Rev. B **92**, 121202 (2015)
15. Y. Ishikawa et al., J. Infrared Milli Terahertz Waves. **39**, 288–301 (2018)
16. Y. Ishikawa et al., J. Infrared Milli Terahertz Waves. **39**, 387–398 (2018)
17. Y. Fujii et al., Appl. Magn. Reson. **49**, 783 (2018)
18. V. Weis et al., J. Magn. Reson. **140**, 293–299 (1999)
19. A.A. Smith et al., J. Magn. Reson. **223**, 170–179 (2012)
20. Y. Ishikawa et al., Appl. Magn. Reson. **52**, 317 (2021)
21. Y. Ishikawa et al., Appl. Magn. Reson. **52**, 305 (2021)
22. L.R. Becerra et al., J. Magn. Reson. Ser. A **117**, 28–40 (1995)
23. C. Caspers et al., APL. Photon. **1**, 026101 (2015)
24. V. Weis, R.G. Griffin, Solid State Nucl. Magn. Reson. **29**, 66–78 (2006)